Spectral LiDAR Analysis for Terrain Classification

Charles A. McIver, Jeremy P. Metcalf, Richard C. Olsen*
Naval Postgraduate School, 833 Dyer Road, Monterey, CA, USA 93943

ABSTRACT

Data from the Optech Titan airborne laser scanner were collected over Monterey, CA, in three wavelengths (532 nm, 1064 nm, and 1550 nm), in May 2016, by the National Center for Airborne LiDAR Mapping (NCALM). Analysis techniques have been developed using spectral technology largely derived from the analysis of spectral imagery. Data are analyzed as individual points, vs techniques that emphasize spatial binning. The primary tool which allows for this exploitation is the N-Dimensional Visualizer contained in the ENVI software package. The results allow for significant improvement in classification accuracy compared to results obtained from techniques derived from standard LiDAR analysis tools.

Keywords: LiDAR, terrain classification, multispectral LiDAR, Optech Titan, point cloud

1. INTRODUCTION

Light detection and ranging (LiDAR) data processing techniques typically use Cartesian coordinate information, infrequently adding intensity from a single wavelength component. Research into the use of multi-wavelength systems for terrain classification is limited and lacks dedicated analysis tools and procedures. The limited prior work are dual-wavelength bathymetric LiDAR studies and a 2016 study by Morsy et al. They used rasterized Optech Titan three-wavelength data, approached by use of three normalized difference feature indices (NDFIs) to conduct separate land vs water and vegetation vs built-up (urban) area classifications in Ontario, Canada[1]. Yu et al (2017) have recently studied the application of Titan data to tree species classification in forest mapping. These authors address intensity variations with range, including corrections for foliage penetration[2].

This research analyzes the contributions to the terrain classification process from a multi-laser (spectral) LiDAR system. Data come from Teledyne Optech's Titan scanner, which provides three-wavelength aerial LiDAR data in 532 nm, 1064 nm, and 1550 nm. Spatial point density is approximately 12 points/m^2. As an important philosophical decision, we do not rasterize our data. Instead, we analyze and classify individual points in the 3-dimensional point cloud comprised of all three wavelengths.

Our objective in this work is to use spectral techniques to analyze the LiDAR data. A heavily validated training set was obtained for the grounds of the Naval Postgraduate School (NPS). Standard analysis approaches were used, starting with a training subset for 5% of the data. Several classification techniques were studied; the focus here is on the use of the Maximum Likelihood (ML) classifier to classify the entire point cloud based on the spectral training regions. The processing approach demonstrated here builds on the earlier works of Thomas[3] and Miller et al.[4]. Refer to McIver[5] for a complete explanation of our data preparations, spectral analysis procedures, classification results, post-processing refinement, and conclusions.

2. DATA

2.1 Sensor

Teledyne Optech's Titan Multispectral LiDAR system, uses three independently-scanning lasers to collect data at a combined ground-sampling rate of 1 MHz. Teledyne states that "the Optech Titan provides greater performance for 3D land cover classification, vegetation mapping, bathymetry, and dense topography"[6]. Titan's three laser channels are as listed: Channel 1 operates in the SWIR at 1550 nanometers (nm). Channel 2 operates in the NIR at 1064 nm. Channel 3 operates in the visible green at 532 nm. The system records all intensities in a 12-bit dynamic range. The 532 nm channel has a beam divergence of ~0.7 mrad; the other two sensors operated at ~0.35 mrad. The other noteworthy difference is in pointing: channel 2 is nadir pointing, channel 1 is pointed 3.5 degrees forward, channel 3 is pointed 7 degrees forward.

*olsen@nps.edu; phone 1 831 656-2019; fax 1 831 656-2834; nps.edu/rsc

Laser Radar Technology and Applications XXII, edited by Monte D. Turner, Gary W. Kamerman, Proc. of SPIE Vol. 10191, 101910J · © 2017 SPIE · CCC code: 0277-786X/17/$18 · doi: 10.1117/12.2276658

2.2 Area of Study

Four of the 28 flight lines collected during NCALM's Monterey, CA flight campaign are selected for this study. Together, these four flight lines (numbers 10, 12, 13, and 15) contain the entire campus of NPS. Each flight line is delivered as three separate LASer (LAS) files, corresponding to one file per channel. A total of 12 LAS v.1.2 files are used. For this study, we are concerned only with the NPS campus, so the four flight lines are cropped to the region shown in Figure 1. Our study area contains 15,022,802 laser points.

Figure 1. NPS campus study area, Monterey, CA in Google Earth.[5]

3. METHODOLOGY

First, we apply several pre-processing steps to merge the separate channels for each flight line into a single-combined LAS file, remove the points at the edges of all flight lines (which are too far apart for spectral incorporation due to the greater scan angle), and clean up point cloud noise. Second, a geometric classifier from the LAStools LiDAR-processing suite[7] is used to commence the classification process by placing all points into four generalized spatially-defined classes: unclassified, ground, vegetation, and buildings. Third, the OpenTStools' nearest-neighbor algorithm[8] accomplishes spectral incorporation by storing the intensity values of every point and its closest neighbors from the other two wavelengths (channels) into the LAS RGB field. Since this occurs with nearly-coincident points, it effectively gives every point three spectral bands: Red-1064 nm, Green-532 nm, and Blue-1550 nm.

Next, the data array is converted from LAS to ASCII format, and ENVI's N-Dimensional Visualizer (N-D VIS) tool[9] is adapted to display the spatial and spectral components of the LiDAR data. In N-D VIS, we develop spectrally-defined regions of interest (ROIs) for a supervised classifier. Our training region consists of a randomly generated 5% subset of data points, evenly dispersed across the study area. The 5% training region is considered our ground truth, which has been vetted by extensive walkthroughs of the study area—our own campus.

3.1 Initial Spatial Classification

LAStools' LASground script classifies all points as ground or not-ground. Heights above ground level (AGL) values are calculated by the LASheight script. LASclassify analyzes apparent surface roughness to classify the not-ground point: planar surfaces as buildings and rough surfaces as vegetation. Points which do not conform to either of these geometric properties remain unclassified. This autonomous spatial classification is limited to approximately 60-70% accuracy, and it only provides four classes. Figure 2 shows the results of LASclassify for an area near Herrmann Hall (the principle building of the school). Notice that the rough roof of clay-tile shingles is often misclassified as vegetation. Also, notice the many points that remain unclassified, especially the building walls and the low-lying shrubs. Although Figure 2 shows only a small segment of campus, these mistakes are characteristic of LASclassify throughout the entire study area.

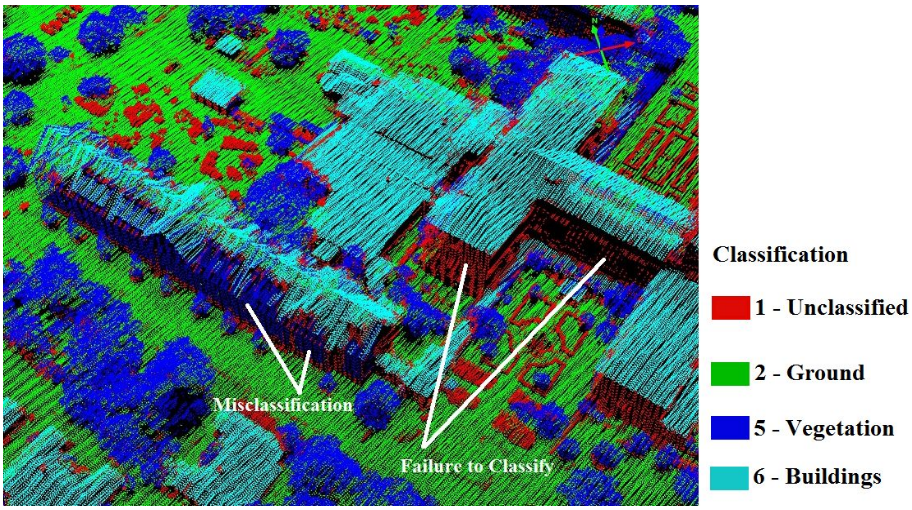

Figure 2. NPS point cloud classified using LAStools' LASclassify tool[5].

3.2 Spectral Incorporation

The nearest neighbor spectral incorporation is accomplished with a locally-developed MATrix LABoratory (MATLAB)[10] script that calls OpenTSTOOL's approximate k-nearest neighbor algorithm. We use Lasdata tools to read and write the LAS files in MATLAB. Figure 3 illustrates how the nearest neighbor process works for every point in all channels: LAS blue field (B) is set to the nearest 1550 nm intensity, red field (R) is set to the nearest 1064 nm intensity, and green field (G) is set to the nearest 532 nm intensity—one of these values will be the point's own intensity, duplicated into the appropriate field.

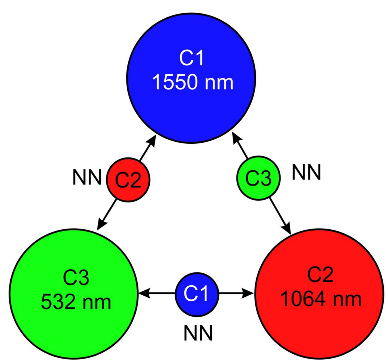

Figure 3. Titan point cloud nearest neighbor RGB attribution[3].

3.3 ENVI Preparation

We convert the data from LAS files to ASCII format with LAStools' las2txt using the flag *–parse xyzirndecauptRGB*. This allows ENVI to read in the LiDAR data as an imagery format without losing any of the LiDAR attributes. The ASCII files are reformatted in Interactive Data Language (IDL) as a modified band sequential (BSQ) interleave (1 x # of points x # of attributes)[4]. To create a training region for the upcoming spectral analysis, we flag a 5% subset of random data points. Table 1 is the list of attributes for every data point—21 spatial/spectral attributes. Three green vegetation indices are calculated from the appropriate RGB intensities according to Table 2[11]. The entire point cloud is saved as an ENVI standard data file with a region of interest (ROI) file, ready for input to N-D VIS using the *visualize with new data* option.

Table 1. List of ASCII point cloud attributes.[4]

Field	Attribute	Field	Attribute
1	X	12	Point Source ID
2	Y	13	GPS Time
3	Z	14	Red *(1064 nm)*
4	Intensity	15	Green *(532 nm)*
5	Return Number	16	Blue *(1550 nm)*
6	Number of Returns	17	Manual Classification
7	Scan Direction	18	Green Normalized Difference Vegetation Index
8	Edge of Flight Line	19	Green Difference Vegetation Index
9	Classification	20	Green Ratio Vegetation Index
10	Scan Angle Rank	21	Reduction Flag
11	Height (AGL) *8-bit relative range*		

Table 2. Vegetation indices calculated.[4]

Index	Formula
Green Normalized Difference Vegetation Index (GNDVI)	GNDVI = (NIR - Green) / (NIR + Green)
Green Difference Vegetation Index (GDVI)	GDVI = NIR - Green
Green Ratio Vegetation Index (GRVI)	GRVI = NIR / Green

3.4 N-D Visualizer

ENVI's n-Dimensional Visualizer tool (N-D VIS) is used to identify ground, vegetation, and building material class clusters and create spectral ROI training classes for input into the Maximum Likelihood supervised classifier[12]. In N-D VIS, we visualize various combinations of the spatial/spectral attributes in Table 1 as bands in an n-dimensional scatterplot. We focus primarily on the RGB spectral bands (14, 15, and 16) for identifying endmember clusters. Viewing the point cloud using bands 1, 2, and 3 (XYZ space) allows us to see the data in a familiar coordinate system.

Data reduction is performed by displaying X (band 1) and reduction flag (band 21) to isolate only the points in the 5% training subset. Selecting X and classification (band 9) allows us to color points according to their LASclassify classifications: unclassified, ground, vegetation, or buildings. This provides the ability to spectrally subclassify the ground, vegetation, and building points separately.

Figure 4 shows ground points only in XYZ and RGB space prior to the definition of endmembers. Figure 5 displays ground points in RGB space after the definition of class clusters. Figure 6 provides the corresponding spectra plots from mean RGB intensities. Figure 7 displays the six new ground classes in XYZ space. AGL is zero for all ground classes.

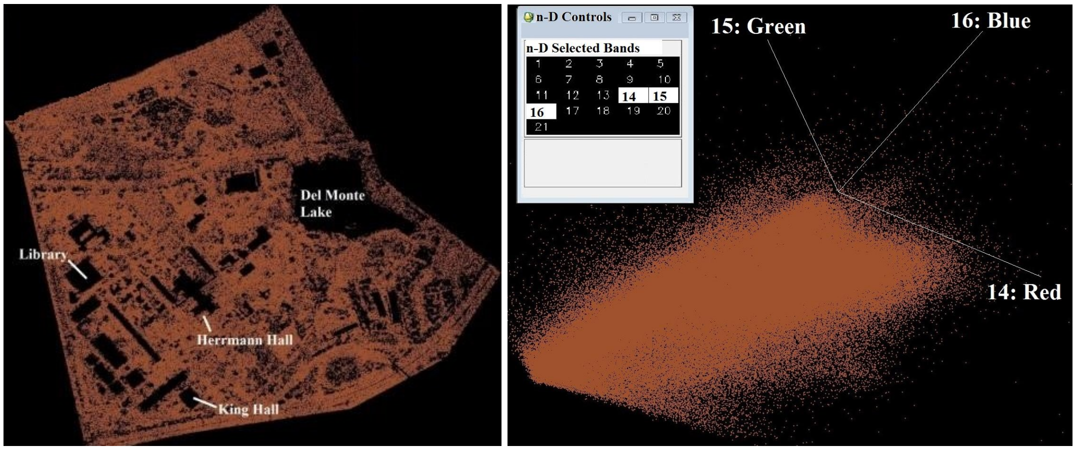

Figure 4. Titan Monterey data—ground points only in XYZ and spectral (RGB) space, prior to sub-classification[5].

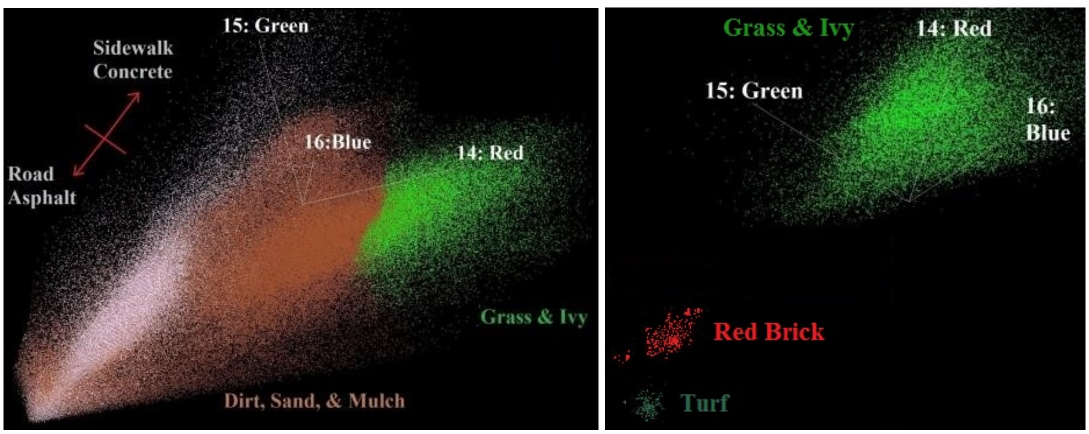

Figure 5. Two screenshots of newly-defined ground classes in N-D VIS RGB space (bands 14, 15, 16)[5].

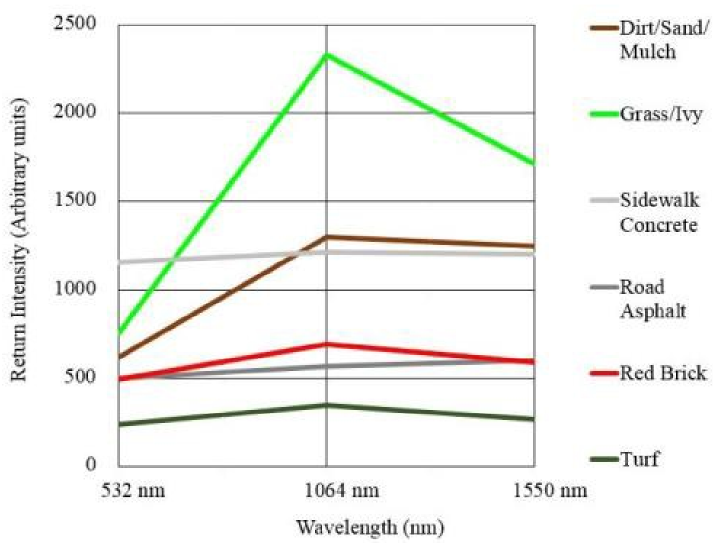

Figure 6. Spectra plots of new ground classes from mean RGB intensities[5].

Figure 7. Titan Monterey data—ground points only in XYZ space, after spectral subclassification[5].

Figure 8 shows the vegetation points in RGB space with the grass, a ground class, displayed as a reference. Vegetation demonstrates mostly lower intensities in all three wavelengths and is difficult to subclassify. Thus, we are only able to divide vegetation loosely into shrubs and trees. Mean AGL for shrubs class is 16.5, and mean AGL for trees is 127.

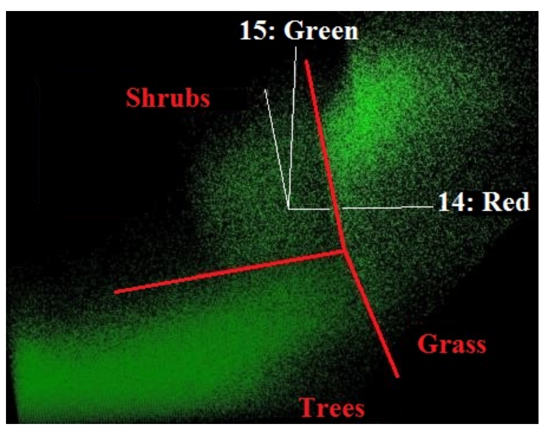

Figure 8. Titan Monterey data—vegetation points (plus grass) in RGB space, after spectral subclassification[5].

Figure 9 shows points from the building class in XYZ and RGB space prior to the definition of endmembers. Figure 10 demonstrates building points in RGB space after the definition of class clusters. Figure 11 provides the corresponding spectra plots from mean RGB intensities and a chart of mean AGLs for each building class. Figure 12 displays the new building classes in XYZ space. To better show the primary roofing materials, Figure 12 excludes the general building class, which is comprised of all leftover building points that do not fit into any of the specific spectral clusters. Finally, Table 3 provides a summary, including point counts, for all of the newly-defined spectral training classes.

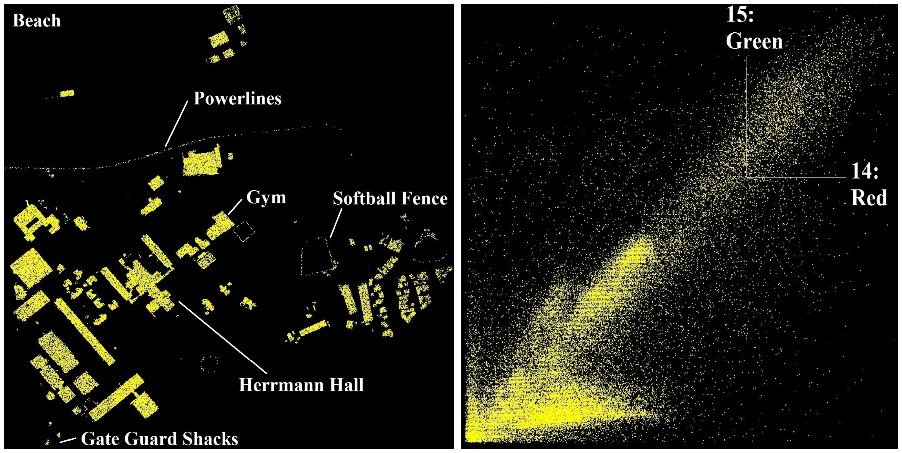

Figure 9. Titan Monterey data—building points in XYZ and RGB space, prior to subclassification[5].

Figure 10. Two screenshots of newly-defined building classes in N-D VIS RGB space[5].

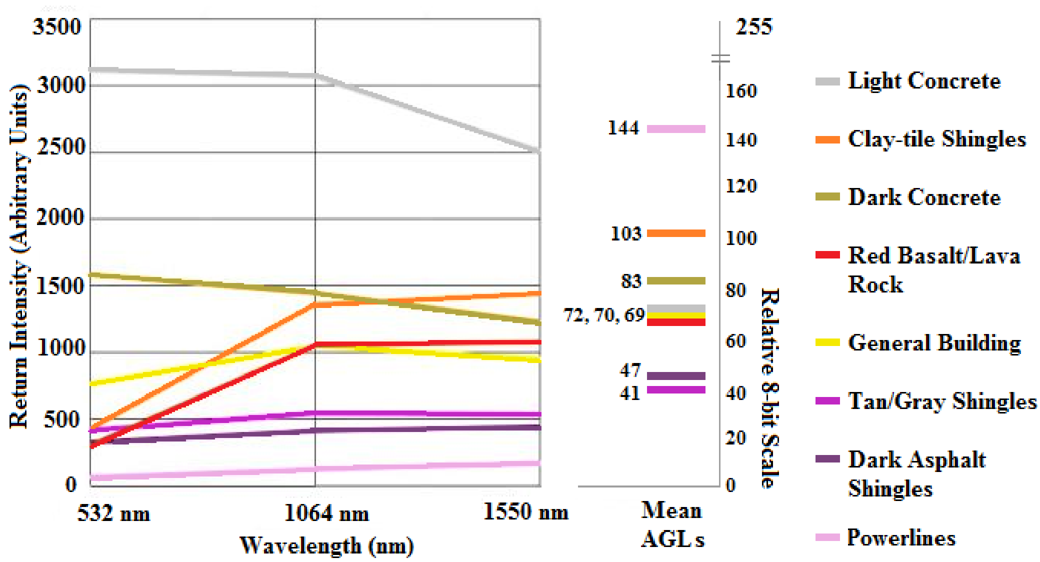

Figure 11. Spectra plots of new building classes from mean RGB intensities and mean AGL plot[5].

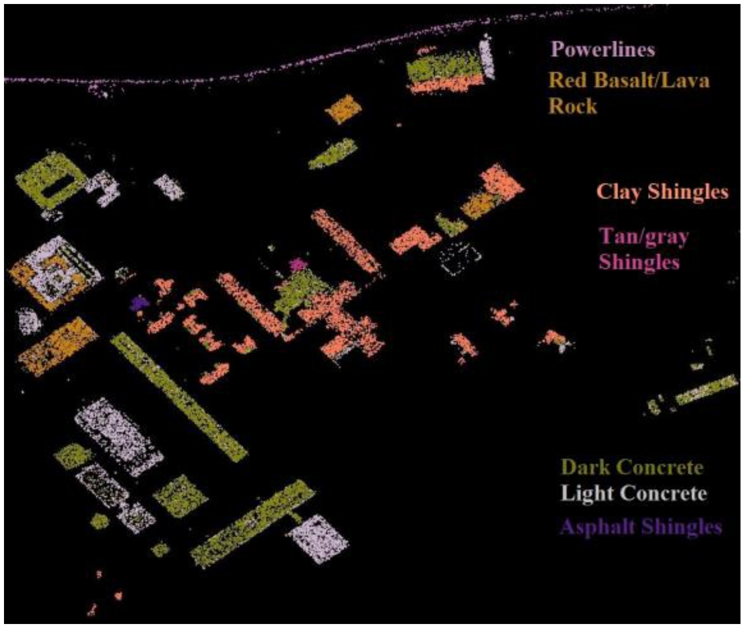

Figure 12. Titan Monterey data—building points only in XYZ space, after spectral subclassification [5].

Table 3. List of Spectral Subclasses Generated Using the 5% Random Subset [5].

New Subclass	Assigned Color	Previous Class—Pre N-D VIS	Number of Points
Dirt, Mulch, & Sand	Sienna	Ground (2)	196,044
Grass & Ivy	Bright Green	Ground (2)	26,204
Sidewalk Concrete	Thistle	Ground (2)	31,872
Road Asphalt	Thistle (Darker)	Ground (2)	72,356
Red Brick	Dark Red	Ground (2)	298
Turf	Sea Green	Ground (2)	122
Shrubs	Middle Green	Vegetation (5)	5,995
Trees	Dark Green	Vegetation (5)	190,083
General Building	Bright Yellow	Building (6)	7,025
Light Concrete	Thistle (Medium)	Building (6)	6,835
Dark Concrete	Yellow/Gold	Building (6)	12,078
Powerlines	Orchid (Pink)	Unclassified (1) & Building (6)	615
Clay-tile Shingles	Coral (orange/pink)	Building (6)	6,799
Tan & Gray Shingles	Magenta	Building (6)	1,313
Dark Asphalt Shingles	Purple	Building (6)	819
Red Basalt & Lava Rock	Dull Orange	Building (6)	2,588

By adding the spectral (RGB) component, we are able to separate the ground points into six subclasses, the vegetation into two subclasses, and the buildings into eight subclasses. We discovered, after the completion of the previous figures and Table 3, that sand can be separated as an additional ground subclass. This brings the total number of ground classes to seven. With the addition of the water class (defined spatially in N-D VIS), 18 total training classes are identified as input ROIs for the Maximum Likelihood classifier.

3.5 Supervised Classification

Maximum Likelihood supervised classification is accomplished using the AGL and RGB attributes of the full-campus point cloud with no probability threshold and 15 of the non-water input classes from Table 3. Sand is separated from the previous dirt, mulch, and sand class. The general building and powerlines classes are discarded as they cause gross misclassifications, especially with tree points.

For each pixel (laser data point), Maximum Likelihood determines a probability value for every class[13]. The class with the highest probability value is then selected as the classification for that pixel, assuming the probability value meets the minimum threshold level for this *most-likely* class[14]. An intermediate rule image is generated for every input class to store the probability values for that class until the classifier is ready to create the final classification image. Figure 13 displays a probability distribution graph for a sample class (concrete – both ground and building). A point's likelihood of being concrete is zero on the right side of the x-axis and progresses to one on the far left. The red and green lines in Figure 13 are representative of the likewise colored points in Figure 14. Figure 14 is a screenshot of the point cloud, where the red and green areas represent those points with a high probability of being classified as concrete.

Figure 15 is a screenshot of the NPS campus, near Herrmann Hall, showing a subset of the results from the Maximum Likelihood classifier. Only the classes that are actually present in the respective area appear in the figure key. Figure 16 displays the entire study area, classified by Maximum Likelihood with all 16 classes.

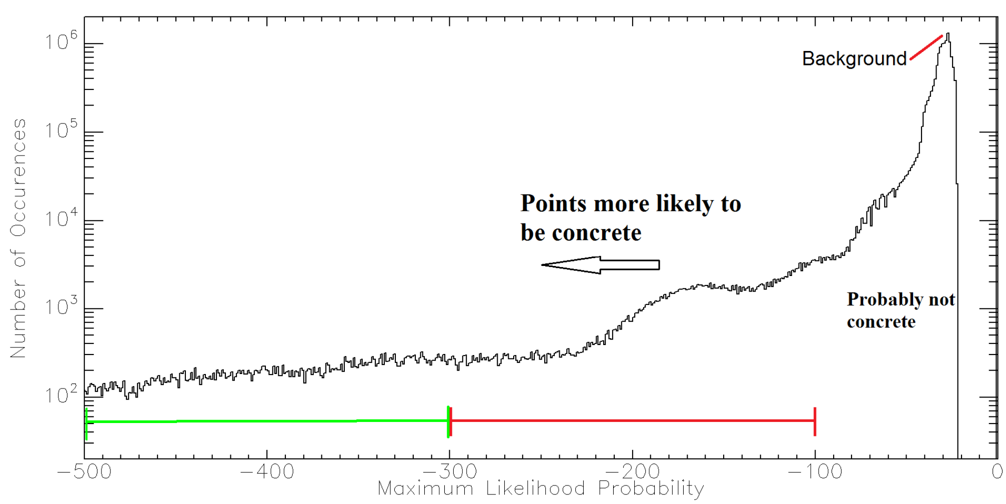

Figure 13. Rule image graph for concrete class showing the probability of each point being concrete[5].

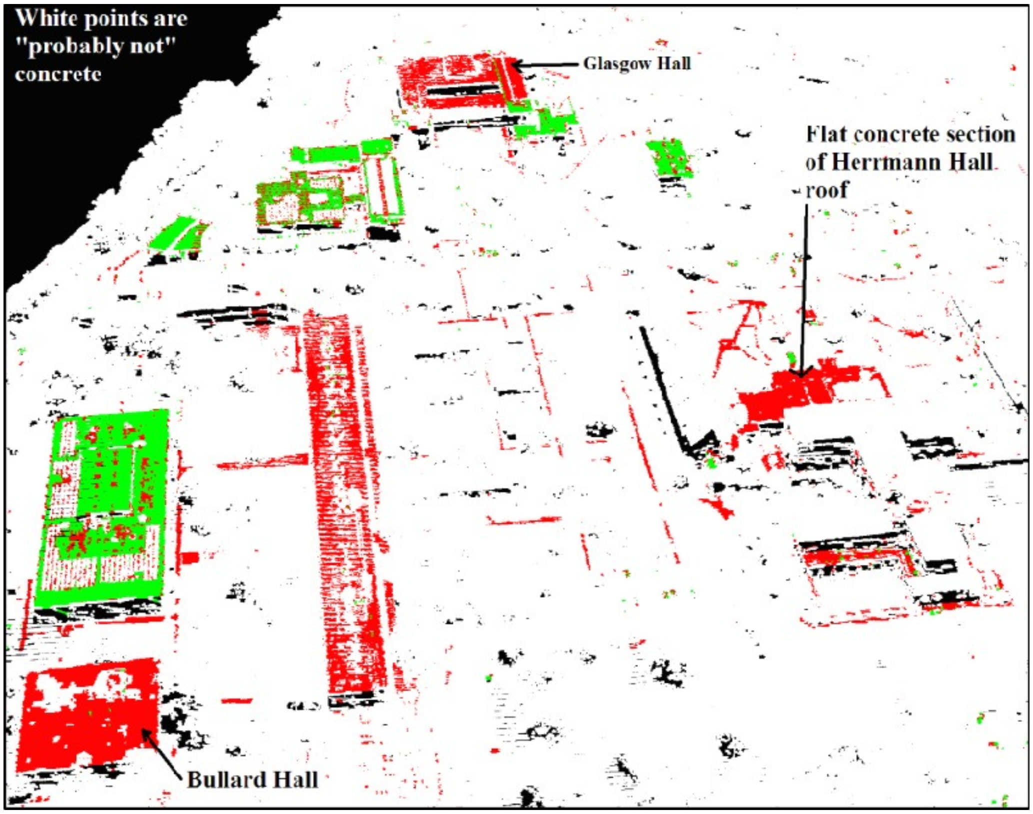

Figure 14. Subarea of NPS point cloud colored according to rule image graph for concrete class[5].

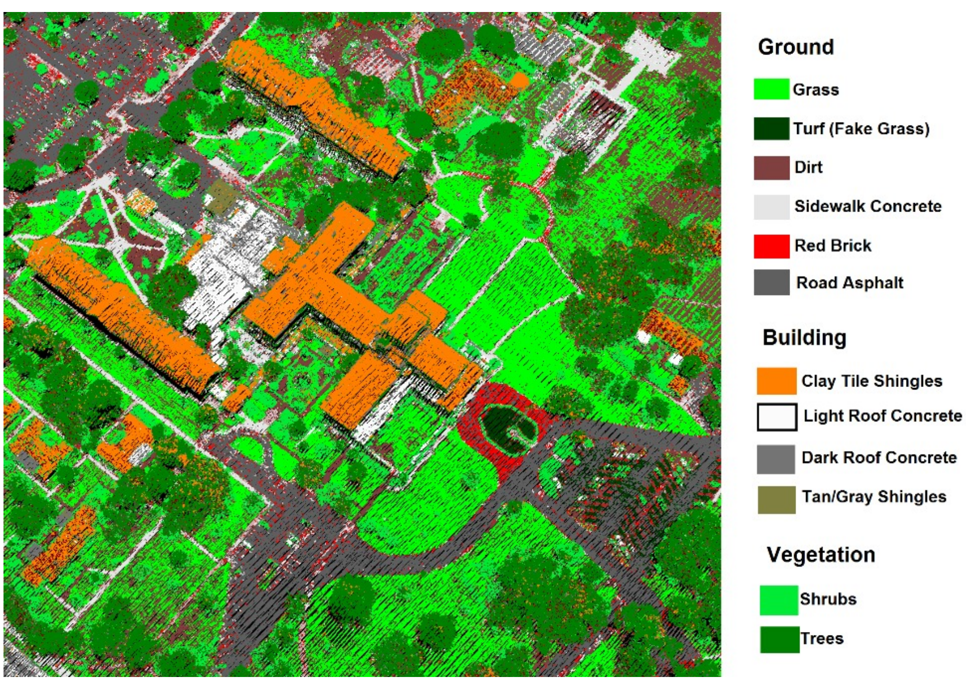

Figure 15. Maximum Likelihood supervised classifier results near Herrmann Hall[5].

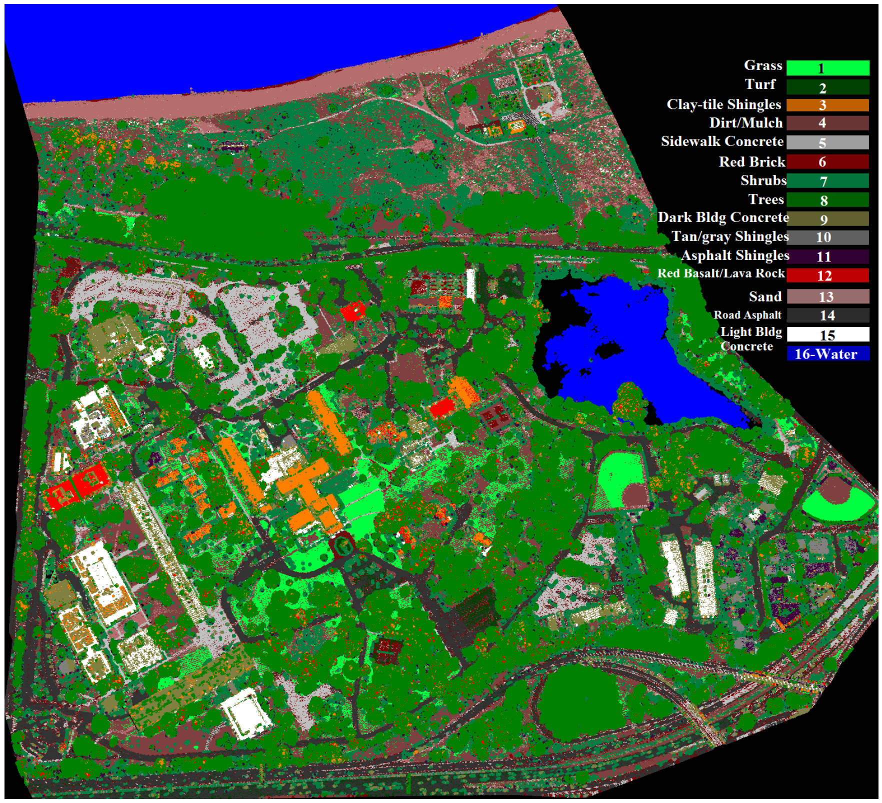

Figure 16. Maximum Likelihood supervised classifier results—full study area[5].

4. RESULTS

The Maximum Likelihood supervised classification results are compared to the manually-classified 5% training subset (Table 4a, 5b, following references) for the following output classes (class number in parenthesis): "grass (# 1), turf (# 2), clay-tile shingles (# 3), dirt and mulch (# 4), sidewalk concrete (# 5), red brick (# 6), shrubs (# 7), trees (# 8), dark building concrete (# 9), tan/gray shingles (# 10), dark asphalt shingles (# 11), red basalt/lava rock (# 12), sand (# 13), road asphalt (# 14), and light building concrete (# 15)" [5]. Table 4 provides the confusion matrix for this ground truth comparison. Class accuracies are in bold-type on the diagonal, and red-text indicates the highest confusion for each class.

Total accuracy is 75%, with grass—99.9% and turf—95% representing the greatest classification successes. The majority of classes have individual accuracies at or better than the total accuracy of 75%. Overall accuracy is largely affected by the 66% individual accuracy of the dirt and mulch class, which contains approximately 22% of all points. The sidewalk concrete class demonstrates the poorest accuracy of 46%, and it is often confused with dirt, sand, and road asphalt. Most classes demonstrate mid-range performances between 70% and 90%

5. CONCLUSIONS

Addition of the spectral LiDAR component increases classification diversity from four classes to 16. Overall classification accuracy is improved over spatial-only methods: 75% vs 60-70%; post-processing using the number-of-returns attribute further improves total accuracy to approximately 80% [5]. It is important to remember that the spectral component is a compliment to, not a substitute for, the point clouds' spatial attributes, such as AGL and number of returns. For example, it is difficult to classify ground and building concretes or trees and shrubs into different classes without the AGL metric.

Spectrally dark (flat signature) materials, such as water, powerlines, and trees, appear too similar and generate a high degree of confusion—especially water points misclassified as vegetation. Water points must be masked or cut-out entirely before classification, and powerlines should not be used as an input training class. Additionally, we may have seen better results in ground classification and overall accuracy by defining a distinct training cluster for dirt and mulch (as we do for sand), instead of leaving the dirt/mulch training class as a somewhat disperse class of the remaining ground points (see Figure 6).

We agree with Miller et al. that Titan's chosen laser channels are ill-suited for vegetation discrimination[4]. The green vegetation indices, in Table 2, provide no considerable improvement to the classification results. A visible red laser is needed to distinguish the IR-ledge ("red edge") and to calculate the traditional vegetation indices in Richards[13]. Unlike Miller et al., this study benefits from easily-accessible ground truth.

This study reinforces two concepts introduced by Thomas[3] and Miller et al.[4]. First, tools designed for the spectral analysis of traditional imagery can be successfully adapted for multi-wavelength LiDAR data. Second, a spectral LiDAR offers a valuable contribution to the terrain classification process over traditional single-wavelength, spatial-only, methods. Future work could apply radiometric correction to the Titan spectral intensities, which may aid in the subclassification of vegetation and other spectrally-dark materials. Based on our high degree of success at spectrally segregating areas of true grass and fake grass (turf), we suggest that future work include analyzing a scene containing various military camouflage setups dispersed among true vegetation.

REFERENCES

[1] Morsy, S., Shaker, A., El-Rabbany, A., and LaRocque, P., "Airborne Multispectral LiDAR Data for Land-cover Classification and Land/Water Mapping Using Different Spectral Indexes," ISPRS Annals of the Photogrammetry, Remote Sensing and Spatial Information Sciences, Vol III-3, (2016).

[2] Yu, X., Hyyppä, J, Litkey, P., Kaartinen, H., Vastaranta, M., Holopainen, M.., "Single-Sensor Solution to Tree Species Classification Using Multispectral Airborne Laser Scanning", Remote Sens, 9(2), p108, (2017),

[3] Thomas, J., "Terrain Classification Using Multi-Wavelength LiDAR Data," (master's thesis, Naval Postgraduate School, 2015). Retrieved from Calhoun http://hdl.handle.net/10945/47337.

[4] Miller, C., Thomas, J., Kim, A., Metcalf, J., and Olsen, R., "Application of image classification techniques to multispectral LiDAR point cloud data," Proc. SPIE 9832, Laser Radar Technology and Applications XXI, 98320X, (2016)

[5] McIver, C., "Spectral LiDAR Analysis and Terrain Classification in a Semi-Urban Environment," (master's thesis, Naval Postgraduate School, 2017). In progress, will be available after June 2017 on Calhoun http://calhoun.nps.edu/.

[6] "Optech Titan Multispectral LiDAR System: High Precision Environmental Mapping," Teledyne Optech, n.d., accessed online at http://www.teledyneoptech.com/wp-content/uploads/Titan-Specsheet-150515-WEB.pdf on 24 March 2017.

[7] Isenburg, M., "LAStools – efficient tools for LiDAR processing" (version 160228, academic), obtained from http://lastools.org.

[8] Merkwirth, C., Parlitz, U., Wedekind, I., Engster, D., and Lauterborn, W., "OpenTSTOOL User Manual," www.physik3.gwdg.de/tstool/.

[9] ENVI version 5.3 + IDL 8.5 (64-bit) classic mode (Harris Geospatial Solutions, Boulder, Colorado).

[10] MATLAB and Statistics Toolbox Release 2015b, The MathWorks, Inc., Natick, Massachusetts, United States.

[11] "Broadband Greenness," Harris Geospatial Solutions, n.d., accessed online at http://www.harrisgeospatial.com/docs/broadbandgreenness.html on 24 March 2017.

[12] "The n-D Visualizer," Harris Geospatial Solutions, n.d., accessed online at http://www.harrisgeospatial.com/docs/nDimensionalVisualizer.html on 26 March 2017.

[13] Richards, J. A., [Remote Sensing Digital Image Analysis: An Introduction], Springer, Berlin, Germany, 194 (2006).

[14] "Maximum Likelihood," Harris Geospatial Solutions, n.d., accessed online at http://www.harrisgeospatial.com/docs/maximumlikelihood.html on 30 March 2016.

Table 4A. Confusion matrix comparing the Maximum Likelihood supervised classifier results to the 5% training subset[5].

	Grass	Turf	Clay-tile	Dirt/Mulch	Sidewalk Concrete	Red Brick	Shrubs
Grass (26,204)	**26,181 (99.9%)**	0	0	23	0	0	0
Turf (122)	1	**116 (95%)**	0	0	0	1	0
Clay-tile Shingles (6,799)	3	0	**5,202 (77%)**	346	1	13	282
Dirt/Mulch (181,865)	16,293	4,262	0	**120,466 (66%)**	4,417	17,258	0
Sidewalk Concrete (31,872)	56	14	0	1,443	**14,657 (46%)**	3,770	0
Red Brick (298)	2	0	0	1	9	**204 (68%)**	0
Shrubs (5,995)	18	3	106	36	0	28	**5,108 (85%)**
Trees (190,083)	0	0	2,902	1	0	0	21,551
Dark Bldg Concrete (12,078)	2	6	212	347	248	841	177
Tan/gray Shingles (1,313)	0	0	9	0	0	0	15
Asphalt Shingles (819)	0	0	0	0	0	0	16
Red Basalt Lava Rock (2,588)	0	0	114	470	0	3	29
Sand (14,179)	0	0	0	228	496	716	0
Road Asphalt (72,356)	0	4,066	0	526	915	5,844	0
Light Bldg Concrete (6,835)	2	0	1	5	37	0	0
Total Accuracy		414,303 of 553,406 points			**75%**		

Table 4B. Confusion matrix comparing the Maximum Likelihood supervised classifier results to the 5% training subset[5] .

	Trees	Dark Bldg Concrete	Tan/gray Shingles	Asphalt Shingles	Red Basalt Lava Rock	Sand	Road Asphalt	Light Bldg Concrete
Grass (26,204)	0	0	0	0	0	0	0	0
Turf (122)	0	0	0	0	0	0	4	0
Clay-tile Shingles (6,799)	48	36	130	0	734	0	2	2
Dirt/Mulch (181,865)	0	1	0	0	0	6,504	12,664	0
Sidewalk Concrete (31,872)	0	0	0	0	0	7,300	4,632	0
Red Brick (298)	0	0	0	0	0	0	82	0
Shrubs (5,995)	301	50	58	178	94	0	7	8
Trees (190,083)	**151,666 (80%)**	1,283	1,729	6,978	3,950	0	0	23
Dark Bldg Concrete (12,078)	25	**7,521 (62%)**	453	10	27	56	150	2,003
Tan/gray Shingles (1,313)	0	8	**1,098 (84%)**	181	2	0	0	0
Asphalt Shingles (819)	3	1	32	**767 (94%)**	0	0	0	0
Red Basalt Lava Rock (2,588)	15	0	22	0	**1,935 (75%)**	0	0	0
Sand (14,179)	0	0	0	0	0	**12,441 (88%)**	298	0
Road Asphalt (72,356)	0	0	0	0	0	130	**60,875 (84%)**	0
Light Bldg Concrete (6,835)	0	724	0	0	0	0	0	**6,066 (89%)**